

Geometry of quantum observables and thermodynamics of small systems

Maxim Olshanii¹

¹*Department of Physics, University of Massachusetts Boston, Boston, MA 02125, USA*

The concept of ergodicity—the convergence of the temporal averages of observables to their ensemble averages—is the cornerstone of thermodynamics. The transition from a predictable, integrable behavior to ergodicity is one of the most difficult physical phenomena to treat; the celebrated KAM theorem is the prime example. This Letter is founded on the observation that for many classical and quantum observables,

the sum of the ensemble *variance* of the temporal average and the ensemble average of temporal *variance* remains constant across the integrability-ergodicity transition.

We show that this property induces a particular geometry of quantum observables—Frobenius (also known as Hilbert-Schmidt) one—that naturally encodes all the phenomena associated with the emergence of ergodicity: the Eigenstate Thermalization effect [1–3], the decrease in the inverse participation ratio [4], and the disappearance of the integrals of motion. As an application, we use this geometry to solve a known problem of optimization of the set of conserved quantities—regardless of whether it comes from symmetries or from finite-size effects—to be incorporated in an extended thermodynamical theory of integrable, near-integrable, or mesoscopic systems [5–9].

Consider a ball in a classical rectangular billiards with periodic boundary conditions, first without and then with a strong localized obstacle inside. (When present, the obstacle makes the system ergodic.) In both cases, consider two kinds of problems: 1. given a specific initial velocity of the ball, what are the subsequent temporal fluctuations in (say) the x -component of the velocity? 2. draw a bunch of initial velocities from a thermal distribution; for each, compute the infinite time average of the x -component of the velocity; what is the variance among these infinite time averages?

If the obstacle is absent, both components of the velocity vector will remain equal to their initial values forever, and so the temporal fluctuations are zero; as far as the second question, the variance of the infinite time averages is equal to that in the thermal distribution, and thus is large. On the other hand, if the obstacle is present, the situation is reversed (this will be so provided the ball keeps hitting the obstacle, which will happen provided the ratio of the velocity components, v_y/v_x , is incommensurate with the ratio of the billiard lengths, L_y/L_x ; and this will hold with probability one as long as the initial velocities as sampled from some continuous probability distribution): now the temporal fluctuations in the velocity component are large no matter what the initial velocity; at the same time, the infinite time average of the velocity component is the same no matter what the initial velocity (namely, it is zero), and so the variance of the infinite time averages is zero. Moreover, as we will show, the shot-to-shot variance in the (exactly integrable) case of an empty billiards equals the temporal variance in the ergodic case.

Given some imagination, one may suspect a “conservation law” acting across the transition from an integrable to an ergodic system as one increases the strength of the integrability-breaking perturbation. Indeed, Fig. 1a shows that in the case of square billiard perturbed by a soft localized potential barrier in the middle [10], the sum of the microcanonical variance of the time average, $\text{Var}_{\text{MC}}[\text{Mean}_t[A]]$, and the shot-to-shot average of the temporal variance, $\text{Mean}_{\text{MC}}[\text{Var}_t[A]]$,

with the observable A being the difference between the horizontal and vertical kinetic energies, remains the same for the heights of the barrier less than or comparable to the kinetic energy. For all points, the statistical ensembles used were microcanonical ensembles with the same phase-space volume ($W = 1184.3$) covered and with the same phase-space volume ($W_b = 7895.7$) occupied by the phase-space points with energies below the lower-energy boundary of the microcanonical window. Such a set of microcanonical ensembles is the closest classical analogue of a quantum set that uses the same window of quantum state *indices* for all perturbation strengths used.

Let us now try to translate the conjecture expressed in the first paragraph of this Letter to quantum language.

Naively, one may try to replace the ensemble of classical initial conditions by an ensemble of random superpositions of quantum eigenstates. However, consider the limiting case of an integrable system. There, a single given initial state will already cover a variety of—generally unrelated—sets of integrals of motion. To the contrary, in the classical case, a given initial point corresponds to a single set. Accordingly, we suggest an ensemble of randomly chosen eigenstates of the Hamiltonian as the ensemble of initial conditions. In particular, the ensemble variance of the temporal means will be translated to the quantum language as

$$\begin{aligned} \text{Var}_{\text{MC}}[\text{Mean}_t[A]] \Big|_{\text{QM}} &\equiv \text{Var}_{\text{MC}}[\langle \alpha | \hat{A} | \alpha \rangle] \\ &= (N_{\text{MC}})^{-1} \sum_{\alpha \in [\text{MC}]} (\langle \alpha | \hat{A} | \alpha \rangle - \langle A \rangle)^2, \quad (1) \end{aligned}$$

where $\langle A \rangle = \text{Mean}_{\text{MC}}[A] \equiv (N_{\text{MC}})^{-1} \sum_{\alpha \in \text{MC}} \langle \alpha | \hat{A} | \alpha \rangle$ is the ensemble mean of the observable \hat{A} , $\sum_{\alpha \in [\text{MC}]} \dots \equiv \sum_{\alpha \in [\alpha_{\min}, \alpha_{\max}]} \dots$ is a sum over a microcanonical window bounded by some energies E_{\min} and E_{\max} , and E_{α} is the energy spectrum of the system. The vanishing of the fluctuations (1) in the thermodynamic limit—the so-called Eigen-

state Thermalization effect—is sufficient [1–3] for the emergence of ergodicity. Our Letter, in part, aims to devise a scale for these fluctuations that determines if a given observable is closer, by behavior, to an integral of motion or to a thermalizable observable.

The question of a proper quantum analogue of the temporal fluctuations is both more involved and better studied. A com-

plication arises from the fact that a quantum state is altered after each measurement. However, consider the following procedure: for every realization of the initial state of interest, the observable is measured only once, and then the initial state is prepared again. For every instant of time of interest, the observable is measured several times, and then, another instant of time is addressed. It has been argued[11] that this

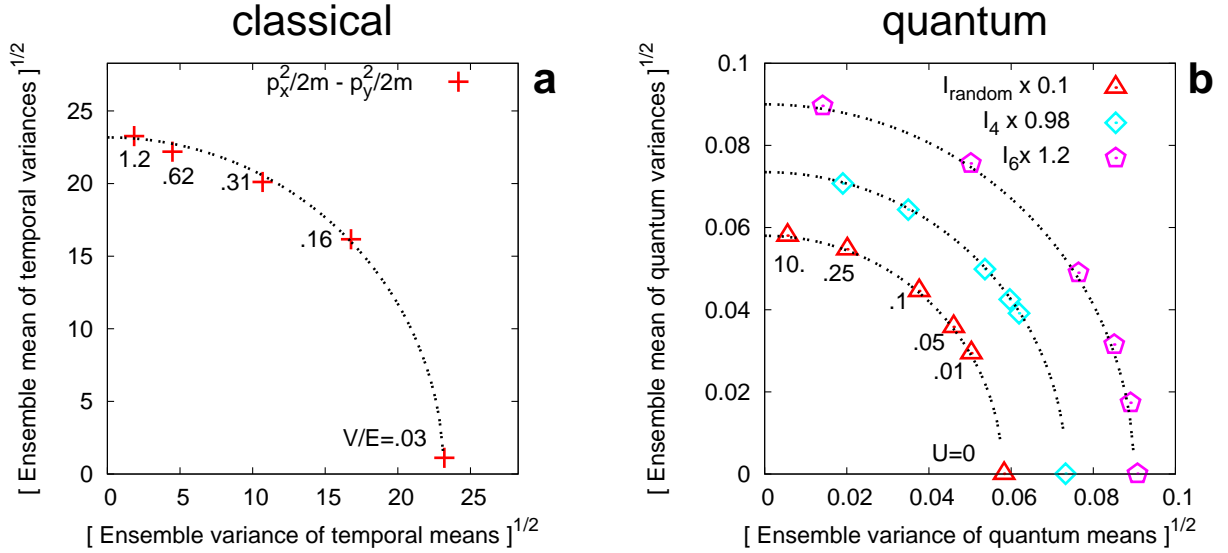


FIG. 1: **Two variances.** The units are such that $m = L/(2\pi) = 1$, where m is the particle mass, and L is the side of the billiard. **a.** Ensemble mean of the temporal variance vs. the ensemble variance of the temporal mean of the difference between the x - and y -kinetic energies for rectangular billiard with periodic boundary conditions perturbed by a soft-core barrier. At zero barrier height, the mean energy over the ensemble is $E_0 = 33.7$. The points plotted are labeled by the ratio, V/E , of the barrier height to the mean energy of the ensemble (that includes the energy of the barrier). **b.** Ensemble mean of the quantum variance vs. the ensemble variance of the quantum expectation values for three integrals of motion of a system of hard core bosons, where the integrals of motion are partially destroyed by adding a soft-core two-body repulsive potential. For this figure: the number of particles is $N = 4$, the number of lattice sites is $L = 16$, and we impose open boundary conditions. The soft-core interaction potential has a constant height U at distances of four sites or less, and it is zero otherwise. I_4 and I_6 (see the text for expressions) are the integrals of motion related to the fourth and sixth moments of the momentum distribution of the underlying free fermions. I_{random} is an artificial integral of motion represented by a diagonal—in the basis of the unperturbed eigenstates—matrix with random entries, uniformly distributed between -1 and $+1$. For this observable, the square cosine of the angle between a point on the figure and the horizontal axis equals (up to small corrections of the order of $(N_{\text{MC}})^{-1}$) the inverse participation ratio η (see Eq. (7)). Observe also that the behavior of the two other observables is qualitatively similar.

procedure is indeed the most suitable quantum counterpart of the classical temporal fluctuations along a trajectory. Furthermore, it has been suggested that in case of an ergodic motion, these fluctuations are nothing else but the *thermal* fluctuations in the system[11]. According to this scenario, the quantum uncertainty in the results of the measurements is the way a quantum system emulates the classical instability with respect to the initial conditions: in both cases, the outcome of a single measurement is irreproducible, fundamentally so in the quantum case, and operationally so in the classical one. Accordingly, we define the quantum analogue of the ensemble mean

of the temporal variance as

$$\begin{aligned} \text{Mean}_{\text{MC}}[\text{Var}_t[A]] \Big|_{\text{QM}} &\equiv \text{Mean}_{\text{MC}}[\langle \alpha | \hat{A}^2 | \alpha \rangle - \langle \alpha | \hat{A} | \alpha \rangle^2] \\ &= (N_{\text{MC}})^{-1} \sum_{\alpha \in [\text{MC}]} \langle \alpha | \hat{A}^2 | \alpha \rangle - \langle \alpha | \hat{A} | \alpha \rangle^2. \end{aligned} \quad (2)$$

Consider now an integrable system, with hamiltonian \hat{H}_0 perturbed by a non-integrable perturbation \hat{V} . The full hamiltonian reads $\hat{H} = \hat{H}_0 + g\hat{V}$, where the parameter g determines the degree by which the integrability is broken. Let the states

$|\alpha\rangle$ be the eigenstates of the full hamiltonian. The conjecture in the first paragraph of the Letter then reads:

$$\begin{aligned} \text{Var}_{\text{MC}}[\text{Mean}_t[A]]\Big|_{\text{QM}} + \text{Mean}_{\text{MC}}[\text{Var}_t[A]]\Big|_{\text{QM}} \\ = \text{a constant independent of } g. \end{aligned} \quad (3)$$

The data presented in Fig. 1b test the conjecture (3) using the example of a one-dimensional gas of lattice hard-core bosons perturbed by an added two-body soft-core repulsive interaction. In one dimension, both continuous-space and lattice hard-core bosons are known to be integrable: in both cases, there is a map (Girardeau’s map[12], and the Jordan-Wigner transformation, respectively) that connects the eigenstates of the system to the eigenstates of a free Fermi gas. The integrals of motion are thus represented by the occupation numbers of the eigenstates of the one body hamiltonian for the particles of the underlying free Fermi gas.

We analyze the decay of the fourth and sixth integrals of motion,

$$\hat{I}_4 = \frac{1}{2L} \sum_{j=1}^{L-2} ((\hat{a}_j^\dagger \hat{a}_{j+2} + h.c.) - (\hat{a}_1^\dagger \hat{a}_1 + \hat{a}_L^\dagger \hat{a}_L)),$$

$$\begin{aligned} \hat{I}_6 = \frac{1}{2L} \sum_{j=1}^{L-3} ((\hat{a}_j^\dagger \hat{a}_{j+3} + h.c.) \\ - ((\hat{a}_1^\dagger \hat{a}_2 + h.c. + (\hat{a}_{L-1}^\dagger \hat{a}_L + h.c.))), \end{aligned}$$

where \hat{a}_j is the j -th site annihilation free-fermionic operator (see also the Supplementary Discussion), as we increase the strength of the non-integrable perturbation. One can see that while the quantum (the analogue of thermal) fluctuations gradually increase, the deviations from the ergodicity decrease. However, in accordance with the conjecture (3), the sum of the two variances remains approximately constant. The square of the radius of the circles corresponds to the ensemble variance of the observable, over a series of *single* measurements—with no subsequent quantum or temporal averaging—on a randomly chosen eigenstate.

Let us now reveal the intuition behind the conjecture (3). The left-hand-side of the relationship (3) can be written, by rearranging the terms in Eqs. 1 and 2, as the *ensemble variance* of the observable \hat{A} :

$$\begin{aligned} \text{Var}_{\text{MC}}[\text{Mean}_t[A]]\Big|_{\text{QM}} + \text{Mean}_{\text{MC}}[\text{Var}_t[A]]\Big|_{\text{QM}} \\ = \text{Mean}_{\text{MC}}[A^2] - \text{Mean}_{\text{MC}}[A]^2. \end{aligned} \quad (4)$$

In turn, the ensemble variance on the right-hand-side of the above equation is a function of two ensemble means; and the key realization is that these ensemble means remain constant as the coupling constant g of the integrability-breaking perturbation is increased from zero up to a value where the system first becomes ergodic. Indeed remark that typically, ergodicity emerges for an interaction strength much weaker than

the one required to alter the thermal expectations of observables. For example, even though the van der Waals interactions between the molecules constituting air do not modify the Maxwell distribution, the interactions are strong enough to lead to a Maxwell distribution from any initial state.

Mathematically, the general criterion for the independence of the ensemble means on g may be stated as follows. For every g , there is a characteristic energy interval $\delta E(g)$ such that the integrability-breaking perturbation appreciably couples only those eigenstates of the integrable hamiltonian whose energy difference is less than $\delta E(g)$. Our criterion is that $\delta E(g)$ be much smaller than the energy width of the microcanonical window used to define the ensemble means. The reason is as follows: consider the eigenstates of the unperturbed system. The perturbation results in their mutual coupling; but if the criterion is fulfilled, then we may neglect the coupling of states within the window to states outside the window. But if we do that, then we may, in fact, truncate our Hilbert space to just the states inside the window (let us call the corresponding hamiltonian a ‘truncated hamiltonian’). Indeed, let us first truncate, and then turn on the perturbation. In that case, the eigenstates of the perturbed truncated hamiltonian are related to those of the unperturbed truncated hamiltonian by a unitary transformation. And now note that the two ensemble means are in fact traces, and thus do not change under unitary transformation of the basis; thus they do not depend on g .

Observe now that in the right hand side of the relationship in Eq. (4), we find a quadratic polynomial, built out of the matrix elements of the observable \hat{A} , that is approximately invariant with respect to changes in the parameter g ; in contrast, on the left-hand side is a sum of two quadratic polynomials that both vary with g . This realization inspires one to seek a geometric meaning of the relationship in Eq. (4), where the right hand side is the square norm of an unknown vector that is linearly related to the operator \hat{A} , and the left hand side is a decomposition of this square norm over some complementary subspaces (that change with the perturbation strength g) of the linear space the vector belongs to. From what follows, we will see that this is almost what happens, with the exception of the $\text{Mean}_{\text{MC}}[A]^2$ term that belongs rather to the left-hand side. The inner product that generates the anticipated geometric structure is the Frobenius, or Hilbert-Schmidt, inner product.

The Frobenius or Hilbert-Schmidt (HS) inner product between two matrices reads:

$$(\hat{A}|\hat{B}) \equiv \text{Tr}[\hat{A}^\dagger \hat{B}]. \quad (5)$$

Quantum observables, represented by Hermitian matrices, form a linear space over the field of real numbers; the product in Eq. (5) induces a real-valued inner product on this space. Observe also that this product is invariant under unitary transformations $\hat{A} \mapsto \hat{U} \hat{A} \hat{U}^{-1}$, where \hat{U} is a unitary matrix. Thus the unitary transformations form a subgroup of all possible linear transformations that preserve the product.

The Hilbert space where we are going to deploy the HS structure is a microcanonical window of eigenstates, of size

for GGE: (a) there are numerical indications that in case of a disorder-induced *localization*, the one-body free-fermionic occupations do not improve the predictive power of thermodynamics at all [9]; (b) not every integrable system can be mapped to free particles; and (c) in the intermediate systems, between integrable and ergodic, the variations of the expectation values of observables from one eigenstate to another are, for all practical purposes, indistinct from the ones generated by well defined integrals of motion. It is therefore desirable to devise a thermodynamic recipe that does not rely on a priori chosen constants of motion. Ideally, one should not even assume that constants of motion exist. The recipe we suggest

is presented below.

To begin, one identifies a linear subspace of observables whose relaxation the generalized ensemble aims to describe. Next, one chooses a diagonal traceless observable that minimizes the Hilbert-Schmidt angle between the space of observables of interest and itself. Next, one repeats the procedure in the space of diagonal traceless observables orthogonal to the first chosen. The procedure is repeated recursively (every time in the space orthogonal to all the integrals of motion previously chosen) till the desired predictive power is reached. This procedure is based on the following exact result and its corollaries, where the HS structure naturally emerges:

$$\text{Var}_{\text{GGE}}[\langle\alpha|\hat{A}|\alpha\rangle] \leq \text{Var}_{\text{MC}}[\langle\alpha|\hat{A}|\alpha\rangle] \left(\sin^2[\theta_{\hat{I}_0, \hat{P}_H \hat{A}_0}] + |\cos[\theta_{\hat{I}_0, \hat{P}_H \hat{A}_0}]| \underbrace{\mathcal{O} \left[\frac{\Delta I}{\sqrt{\text{Var}_{\text{MC}}[\langle\alpha|\hat{I}|\alpha\rangle]}} \right]}_{\ll 1} \right), \quad (8)$$

where \hat{P}_H is a “super-operator” that removes the off-diagonal (with respect to the basis of the eigenstates of \hat{H}) matrix elements, $\Delta I \equiv \max_j(I_{j+1} - I_j)$ is the maximal width of the microcanonical window for the additional integral of motion, and $\{[I_{j+1} - I_j]\}$ is a set of intervals tiling the axis of the integral of motion I . (See the extensive discussion in Supplementary Material [10].) Here and below, $\text{Var}_{\text{GGE}}[\langle\alpha|\hat{A}|\alpha\rangle]$ and $\text{Var}_{\text{MC}}[\langle\alpha|\hat{A}|\alpha\rangle]$ define the mean square error of the (microcanonical version of) GGE and of the microcanonical ensemble proper.

Figure 3 shows the result of an application of this procedure to another system of one-dimensional hard-core bosons, smaller than before so that finite-size effects are enhanced. The space of observables of interest was formed by all distinct matrix elements of the one-body density matrix. We analyze the momentum distribution, considering both the integrable case (Figs. 3a,c) and the case where the integrability is broken by a soft-core finite-range repulsive potential (Figs. 3b,d). We compare three thermodynamical ensembles. The first one is the traditional microcanonical ensemble. The second is a generalized microcanonical ensemble that fixes not only the value of the energy but generally all one-body occupation numbers of the underlying free-fermionic system (or, in the nonintegrable case, their time-averaged values). The third is an ensemble based on the first few most relevant integrals of motion chosen using the Hilbert-Schmidt optimization procedure. Fig. 3c demonstrates that in the integrable case, the accuracy of the second and the third ensembles are com-

parable while both greatly exceed the one of the conventional thermal ensemble. This indicates that the free-fermionic integrals of motion are indeed the optimal predictors of the after-relaxation state of the system in this case. However, the free-fermionic one-body occupations are not available at all in the perturbed case (see Fig. 3d). Nevertheless, the optimized generalized microcanonical ensemble remains well defined, and it fully retains its predictive power. Remark that for the strength of perturbation chosen, the system remains relatively close to integrable, showing a high inverse participation ratio of $\eta = .29$.

Finally, in Fig. 4 we consider a quench from the ground state in the integrable regime to a strongly perturbed regime ($\eta = .023$). Here we directly compare the infinite time average with the predictions of both the microcanonical and the optimal GGE ensembles. The predictive power of the latter is indeed higher than of the former.

Two distinct sources of deviation from the thermal behavior are traditionally identified. The first, the mathematically elegant one, is associated with either nontrivial symmetries or with the Bethe ansatz [16, 17]. The second source, the empirically important, stems from the deviations from the Eigenstate Thermalization [3] in finite systems. In small systems,—such as the nano-opto-mechanical resonators [18–24]—the two become practically indistinct, and no obvious candidates for the relevant conserved quantities are any longer visible: here, our theory offers a unified approach, based on a “blind” optimization of the predictive power of thermodynamics.

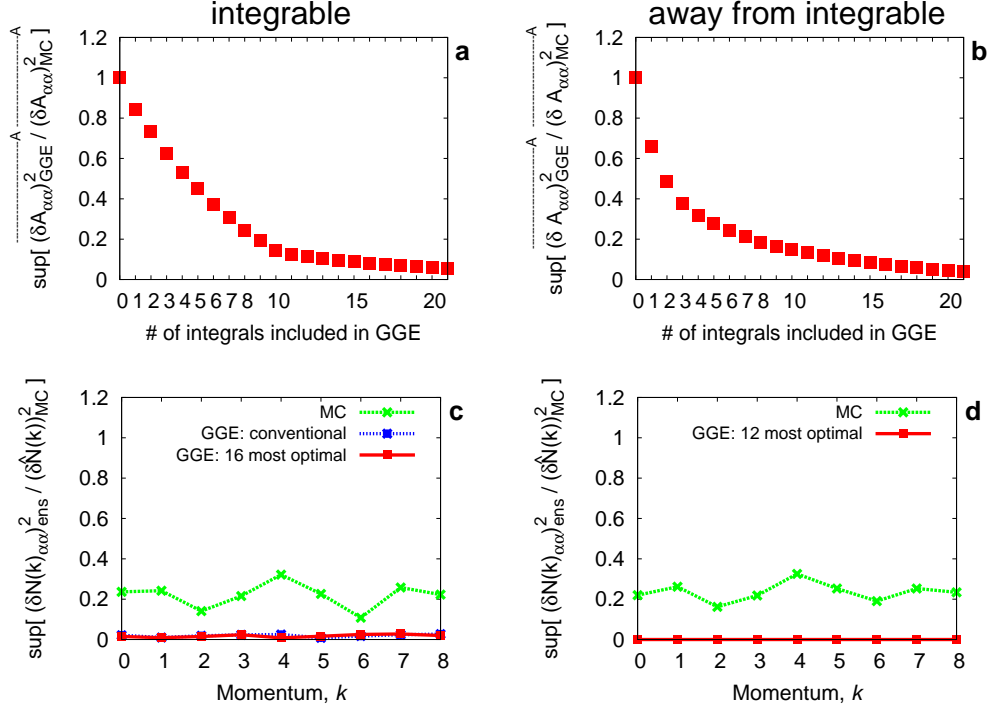


FIG. 3: **Predictive power of two extensions of the microcanonical ensemble.** We use the example of a system of one-dimensional hard-core bosons. For this figure: the number of particles is $N = 3$, we use periodic boundary conditions, and the rest of the parameters is the same as for Fig. 1b. **a**, An upper bound [10] on the mean-square error of the predictions of the Generalized Gibbs Ensemble, optimal with respect to all one-body observables (the optimal GGE), as a function of the allowed number of the additional integrals of motion involved. The error of the standard microcanonical (MC) ensemble is used as a reference. We consider the integrable case, $U = 0$. The result is averaged over all one-body observables. **b**, The same as for **a**, but away from integrability, with $U = .1$. **c**, An upper bound on the mean-square error of the predictions of the optimal GGE, for the momentum distribution, in the integrable case ($U = 0$). The number of the integrals of motion is fixed to the number of lattice sites, $L = 16$. The results for the microcanonical ensemble, and for the conventional free-fermionic Generalized Gibbs Ensemble (GGE)[5] are shown for comparison. The ensemble variance of the observables is used as a reference. **d**, The same as for **c**, but with $U = .1$. Note that in the nonintegrable case, no free theory is available for comparison.

SUPPLEMENTARY DISCUSSION

1. Two lemmas used to establish the upper bounds on the accuracy of the Generalized Gibbs Ensembles.

Lemma 1. Let \hat{q} be a real $n \times n$ matrix of orthogonal projection (i.e. let \hat{q} be idempotent and symmetric: $\hat{q}\hat{q} = \hat{q}$ and $\hat{q} = \hat{q}^T$, where T denotes transposition). Then for any two n -dimensional real vectors \vec{a} and \vec{v} ,

$$\|\hat{q}\vec{a}\|^2 \leq \|\vec{a}\|^2 \left\{ \sin^2[\theta_{\vec{v}, \vec{a}}] + 2|\cos[\theta_{\vec{v}, \vec{a}}]| \frac{\|\hat{q}\vec{v}\|}{\|\vec{v}\|} \right\}, \quad (9)$$

where $\theta_{\vec{v}_1, \vec{v}_2}$ is the angle between two vectors \vec{v}_1 and \vec{v}_2 , i.e. $\theta_{\vec{v}_1, \vec{v}_2} \equiv \arccos[(\vec{v}_1 \cdot \vec{v}_2)/(\|\vec{v}_1\|\|\vec{v}_2\|)]$ and $0 \leq \theta_{\vec{v}_1, \vec{v}_2} \leq \pi$, and $\|\vec{v}\| \equiv \sqrt{(\vec{v} \cdot \vec{v})}$ is the norm of a vector \vec{v} .

Proof. Let $\hat{p} \equiv \hat{1} - \hat{q}$ be the orthogonal projection complementary to \hat{q} . Similarly to \hat{q} , it is idempotent and symmetric. Any vector \vec{v} can be decomposed onto the sum $\vec{v} = \hat{p}\vec{v} + \hat{q}\vec{v}$, with $(\hat{p}\vec{v} \cdot \hat{q}\vec{v}) = 0$. As a consequence, $\|\vec{v}\|^2 = \|\hat{p}\vec{v}\|^2 + \|\hat{q}\vec{v}\|^2$.

The proof goes as follows:

$$\begin{aligned} \|\hat{q}\vec{a}\|^2 &= \|\vec{a}\|^2 - \|\hat{p}\vec{a}\|^2 \quad (\text{using } \|\vec{a}\|^2 = \|\hat{p}\vec{a}\|^2 + \|\hat{q}\vec{a}\|^2) \\ &\stackrel{\text{CSI}}{\leq} \|\vec{a}\|^2 - \frac{(\vec{v} \cdot \hat{p}\vec{a})^2}{\|\vec{v}\|^2} \\ &= \|\vec{a}\|^2 - \frac{(\hat{p}\vec{v} \cdot \vec{a})^2}{\|\vec{v}\|^2} \quad (\text{using that } \hat{p} \text{ is symmetric}) \\ &= \|\vec{a}\|^2 - \frac{((\vec{v} \cdot \vec{a}) - (\hat{q}\vec{v} \cdot \vec{a}))^2}{\|\vec{v}\|^2} \quad (\text{using } \hat{p} = \hat{1} - \hat{q}) \\ &\stackrel{\text{RTI}}{\leq} \|\vec{a}\|^2 - \frac{(|(\vec{v} \cdot \vec{a})| - |(\hat{q}\vec{v} \cdot \vec{a})|)^2}{\|\vec{v}\|^2} \\ &= \|\vec{a}\|^2 - \frac{(\vec{v} \cdot \vec{a})^2 - 2|(\vec{v} \cdot \vec{a})||(\hat{q}\vec{v} \cdot \vec{a})| + (\hat{q}\vec{v} \cdot \vec{a})^2}{\|\vec{v}\|^2} \\ &\leq \|\vec{a}\|^2 - \frac{(\vec{v} \cdot \vec{a})^2 - 2|(\vec{v} \cdot \vec{a})||(\hat{q}\vec{v} \cdot \vec{a})|}{\|\vec{v}\|^2} \\ &\stackrel{\text{CSI}}{\leq} \|\vec{a}\|^2 - \frac{(\vec{v} \cdot \vec{a})^2 - 2|(\vec{v} \cdot \vec{a})||\hat{q}\vec{v}||\|\vec{a}\|}{\|\vec{v}\|^2} \\ &= \|\vec{a}\|^2 \left\{ \sin^2[\theta_{\vec{v}, \vec{a}}] + 2|\cos[\theta_{\vec{v}, \vec{a}}]| \frac{\|\hat{q}\vec{v}\|}{\|\vec{v}\|} \right\}. \end{aligned}$$

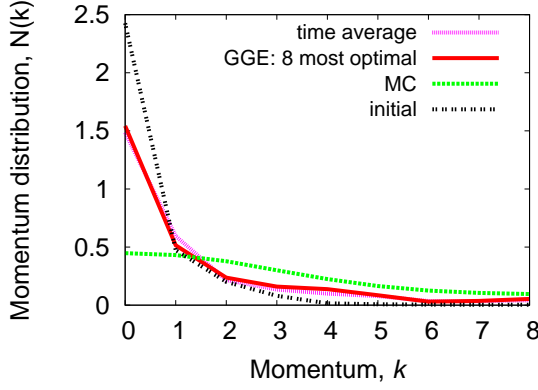


FIG. 4: **Momentum distribution after a quench from the ground state of another hamiltonian.** The initial state is the ground state of a hard-core boson hamiltonian for $N = 4$ atoms on $L = 16$ sites, with periodic boundary conditions. At $t = 0+$, a soft-core repulsion of strength $U = 3$ is turned on. The microcanonical ensemble is represented by $N_{\text{MC}} = 300$ lowest eigenstates. The GGE ensemble incorporates the values of 8 most optimal integrals of motion. Each integral of motion (except the first, which was strongly correlated with the energy) was fixed to a window around its initial state value. The half-width of each window was 10% of the corresponding microcanonical standard deviation.

□

Here, CSI stands for the Cauchy-Schwarz inequality, $|(\vec{v}_1 \cdot \vec{v}_2)| \leq \|\vec{v}_1\| \|\vec{v}_2\|$, and RTI denotes the reverse triangle inequality, $|x - y| \leq \|x\| - \|y\|$, x and y being real numbers.

Lemma 2. For any two real numbers α and σ ,

$$\|\vec{a}_\perp + \alpha\vec{u}\|^2 \sin^2[\theta_{\vec{v}_\perp + \sigma\vec{u}, \vec{a}_\perp + \alpha\vec{u}}] \geq \|\vec{a}_\perp\|^2 \sin^2[\theta_{\vec{v}_\perp, \vec{a}_\perp}], \quad (10)$$

where $\vec{a}_\perp, \vec{v}_\perp$ are real n -dimensional vectors, \vec{u} is a real unit n -dimensional vector, $\|\vec{u}\| = 1$, and $(\vec{a}_\perp \cdot \vec{u}) = (\vec{v}_\perp \cdot \vec{u}) = 0$.

Proof. Since neither the left- nor the right-hand-side of the inequality (10) depends on the norm of \vec{v} , we may assume, without loss of generality, that \vec{v} is a unit norm vector: $\vec{v} = \vec{e}_\vec{v}$, where $\|\vec{e}_\vec{v}\| = 1$. It can be further decomposed as $\vec{e}_\vec{v} = \cos(\eta)(\vec{e}_\vec{v})_\perp + \sin(\eta)\vec{u}$, where $(\vec{e}_\vec{v})_\perp \equiv \vec{e}_\vec{v} - (\vec{u} \cdot \vec{e}_\vec{v})\vec{u}$. The

proof is as follows:

$$\begin{aligned} \|\vec{a}_\perp + \alpha\vec{u}\|^2 \sin^2[\theta_{\vec{v}_\perp, \vec{a}_\perp + \alpha\vec{u}}] &\stackrel{\vec{v}=\vec{e}_\vec{v}}{=} \|\vec{a}_\perp + \alpha\vec{u}\|^2 \sin^2[\theta_{\vec{e}_\vec{v}, \vec{a}_\perp + \alpha\vec{u}}] \\ &\stackrel{\vec{v}=\vec{e}_\vec{v}}{=} \|\vec{a}_\perp + \alpha\vec{u}\|^2 - (\vec{e}_\vec{v} \cdot (\vec{a}_\perp + \alpha\vec{u}))^2 \\ &= \|\vec{a}_\perp\|^2 - (\vec{e}_\vec{v} \cdot \vec{a}_\perp)^2 + (1 - (\vec{e}_\vec{v} \cdot \vec{u})^2)\alpha^2 \\ &\quad - 2(\vec{e}_\vec{v} \cdot \vec{a}_\perp)(\vec{e}_\vec{v} \cdot \vec{u})\alpha \\ &\geq \|\vec{a}_\perp\|^2 - (\vec{e}_\vec{v} \cdot \vec{a}_\perp)^2 \\ &\quad + \min_\alpha \left[\underbrace{(1 - (\vec{e}_\vec{v} \cdot \vec{u})^2)}_{\geq 0} \alpha^2 - 2(\vec{e}_\vec{v} \cdot \vec{a}_\perp)(\vec{e}_\vec{v} \cdot \vec{u})\alpha \right] \\ &= \|\vec{a}_\perp\|^2 - (\vec{e}_\vec{v} \cdot \vec{a}_\perp)^2 - \frac{(\vec{e}_\vec{v} \cdot \vec{a}_\perp)^2 (\vec{e}_\vec{v} \cdot \vec{u})^2}{1 - (\vec{e}_\vec{v} \cdot \vec{u})^2} \\ &= \|\vec{a}_\perp\|^2 - \frac{(\vec{e}_\vec{v} \cdot \vec{a}_\perp)^2}{1 - (\vec{e}_\vec{v} \cdot \vec{u})^2} \\ &= \|\vec{a}_\perp\|^2 - \frac{\cos^2[\eta] ((\vec{e}_\vec{v})_\perp \cdot \vec{a}_\perp)^2}{1 - \sin^2[\eta]} \\ &\quad (\text{using } \vec{e}_\vec{v} = \cos(\eta)(\vec{e}_\vec{v})_\perp + \sin(\eta)\vec{u}) \\ &= \|\vec{a}_\perp\|^2 - ((\vec{e}_\vec{v})_\perp \cdot \vec{a}_\perp)^2 \\ &= \|\vec{a}_\perp\|^2 \sin^2[\theta_{\vec{v}_\perp, \vec{a}_\perp}]. \quad (\text{using } (\vec{e}_\vec{v})_\perp = \vec{v}_\perp) \end{aligned}$$

□

2. Accuracy of a Generalized Gibbs Ensemble. A single additional integral of motion and a single observable of interest.

Imagine that we are interested in predicting the infinite time average of the quantum-mechanical mean of an observable \hat{A} , given the initial state. According to the standard microcanonical scenario, the energy scale is divided onto narrow intervals, $[E_i, E_{i+1}]$. The only information about the initial state we are given is which energy interval, i^* , the quantum expectation value of the energy belongs to. The microcanonical prediction for the time average of the observable in the subsequent evolution is

$$\begin{aligned} \text{Prediction}[\text{Mean}_t[A]] &= \text{Mean}_{\text{MC}}[A] \\ &= \frac{\sum_{\alpha \in D_{i^*}} \langle \alpha | \hat{A} | \alpha \rangle}{\sum_{\alpha \in D_{i^*}} 1}, \end{aligned}$$

where D_i is the interval of the eigenstate indices α populated by the eigenstates whose energy belongs to the interval $[E_i, E_{i+1}]$:

$$\alpha \in D_i \Leftrightarrow E_\alpha \in [E_i, E_{i+1}]. \quad (11)$$

Now, assume that in the initial state, the system's energy is measured exactly, yielding a value E_{α^*} , but the only information we get is, again, the interval D_{i^*} this energy belongs to. Assuming that within the interval D_{i^*} each eigenstate can appear with equal probability, the mean square error of the microcanonical prediction for the quantum-mechanical mean

of \hat{A} is

$$\text{Var}_{\text{MC}}[\langle \alpha | \hat{A} | \alpha \rangle] = \frac{\sum_{\alpha \in D_{i^*}} (\langle \alpha | \hat{A} | \alpha \rangle - \text{Mean}_{\text{MC}}[A])^2}{\sum_{\alpha \in D_{i^*}} 1}.$$

The vanishing of this variance in the thermodynamic limit is the essence of the Eigenstate Thermalization Hypothesis [1–3].

Imagine now that we are given an extra piece of information: via a second measurement in the initial state, we are allowed to place another integral of motion \hat{I} —an observable with all off-diagonal matrix elements equal to zero—to an interval j^* , one of a set of intervals $[I_j, I_{j+1}]$. An ensemble of states with $E_\alpha \in [E_{i^*}, E_{i^*+1}]$ and $I_\alpha \in [I_{j^*}, I_{j^*+1}]$, distributed with equal probability, forms a minimal version of the Generalized Gibbs Ensemble [5]. Its prediction for the quantum mean of the observable \hat{A} reads:

$$\begin{aligned} \text{Prediction}[\text{Mean}_t[A]] &= \text{Mean}_{\text{GGE}|j^*}[A] \\ &= \frac{\sum_{\alpha \in D_{i^*} \cap S_{j^*}} \langle \alpha | \hat{A} | \alpha \rangle}{\sum_{\alpha \in D_{i^*} \cap S_{j^*}} 1}, \end{aligned}$$

$$\text{MSE}[\text{Prediction}[\text{Mean}_t[A]]] \equiv \text{Var}_{\text{GGE}}[\langle \alpha | \hat{A} | \alpha \rangle] \leq$$

$$\text{Var}_{\text{MC}}[\langle \alpha | \hat{A} | \alpha \rangle] \left(\sin^2[\theta_{\hat{I}_t, \hat{P}_H \hat{A}_t}] + |\cos[\theta_{\hat{I}_t, \hat{P}_H \hat{A}_t}]| \mathcal{O} \left[\underbrace{\frac{\Delta I}{\sqrt{\text{Var}_{\text{MC}}[\langle \alpha | \hat{I} | \alpha \rangle]}}}_{\ll 1} \right] \right), \quad (12)$$

where $\theta_{\hat{B}_1, \hat{B}_2}$ is the Hilbert-Schmidt angle between the observables \hat{B}_1 and \hat{B}_2 , a traceless version of a given observable, \hat{B} , is defined as $\hat{B}_t \equiv \hat{B} - \text{Tr}[\hat{B}]/N_{\text{MC}}$, \hat{P}_H is a “super-operator” that removes the off-diagonal (with respect to the basis of the eigenstates of \hat{H}) matrix elements, and $\Delta I \equiv \max_j(I_{j+1} - I_j)$ is the maximal width of a microcanonical window for the additional integral of motion.

The estimate in Eq. (12) shows that the biggest increase in the predictive power of the Generalized Gibbs Ensemble is delivered by the integrals of motion at a small Hilbert-Schmidt angle to the observable of interest. To the dominant order in the size of the microcanonical boxes for the integral of motion ΔI , the bound does not depend on the details of the partition of the axis of the integral of motion I .

Remark that if the bound (12) is used to assess the accuracy in a quench from a linear superposition of the eigenstates, the variance of the integral of motion in the initial state must be smaller than ΔI .

The dictionary used to relate Lemma 1 to the bound (12) is

where

$$\alpha \in S_j \Leftrightarrow I_\alpha \in [I_j, I_{j+1}].$$

Here and below, $I_\alpha \equiv \langle \alpha | \hat{I} | \alpha \rangle$.

The predictions of the new ensemble are, by construction, always more accurate than the microcanonical ones. Using Lemma 1 from Sec. 1, one can prove the following

Theorem. *In predicting the infinite time average of an observable \hat{A} , the mean square error (MSE) of the prediction of Generalized Gibbs Ensemble based on an integral of motion \hat{I} ,*

$$\begin{aligned} \text{MSE}[\text{Prediction}[\text{Mean}_t[A]]] &\equiv \text{Var}_{\text{GGE}}[\langle \alpha | \hat{A} | \alpha \rangle] \\ &= \frac{\sum_j \sum_{\alpha \in D_{i^*} \cap S_j} (\langle \alpha | \hat{A} | \alpha \rangle - \text{Mean}_{\text{GGE}|j}[A])^2}{\sum_{\alpha \in D_{i^*}} 1}, \end{aligned}$$

(where it is assumed that the initial states are still uniformly distributed inside $[E_{i^*}, E_{i^*+1}]$) is bounded from the above as

as follows:

$$\begin{aligned} \vec{a} &\rightarrow \{\langle \alpha | \hat{A} | \alpha \rangle \mid \alpha \in D_{i^*}\} \\ \vec{v} &\rightarrow \{\langle \alpha | \hat{I} | \alpha \rangle \mid \alpha \in D_{i^*}\} \\ \hat{q}\vec{a} &\rightarrow \{\langle \alpha | \hat{A} | \alpha \rangle - \text{Mean}_{\text{GGE}|j(\alpha)}[A] \mid \alpha \in D_{i^*}\} \\ \hat{q}\vec{v} &\rightarrow \{\langle \alpha | \hat{I} | \alpha \rangle - \text{Mean}_{\text{GGE}|j(\alpha)}[I] \mid \alpha \in D_{i^*}\} \\ \|\vec{a}\|^2 &\rightarrow \text{Var}_{\text{MC}}[\langle \alpha | \hat{A} | \alpha \rangle] + \text{Mean}_{\text{MC}}[A]^2 \\ \|\vec{v}\|^2 &\rightarrow \text{Var}_{\text{MC}}[\langle \alpha | \hat{I} | \alpha \rangle] + \text{Mean}_{\text{MC}}[I]^2 \\ \|\hat{q}\vec{a}\|^2 &\rightarrow \text{Var}_{\text{GGE}}[\langle \alpha | \hat{A} | \alpha \rangle] \\ \|\hat{q}\vec{v}\|^2 &\rightarrow \text{Var}_{\text{GGE}}[\langle \alpha | \hat{I} | \alpha \rangle]. \end{aligned}$$

Lemma 2 shows that the first term of the bound in Eq. (9) (which is the dominant term in our context) can be further improved by removing a component along a particular unit vector \vec{u} . In our case, the role of the vector \vec{u} will be played by a Hilbert-Schmidt-normalized identity operator. The following

dictionary completes the proof of Eq. (12):

$$\begin{aligned}
\vec{a}_\perp &\rightarrow \{\langle \alpha | \hat{A}_\perp | \alpha \rangle \mid \alpha \in D_{i^*}\} \\
\vec{v}_\perp &\rightarrow \{\langle \alpha | \hat{I}_\perp | \alpha \rangle \mid \alpha \in D_{i^*}\} \\
\vec{u} &\rightarrow \{1/\sqrt{N_{\text{MC}}} \mid \alpha \in D_{i^*}\} \\
\|\vec{a}_\perp\|^2 &\rightarrow \text{Var}_{\text{MC}}[\langle \alpha | \hat{A} | \alpha \rangle] \\
\|\vec{v}_\perp\|^2 &\rightarrow \text{Var}_{\text{MC}}[\langle \alpha | \hat{I} | \alpha \rangle] \\
\|\hat{q}\vec{a}_\perp\|^2 &\rightarrow \text{Var}_{\text{GGE}}[\langle \alpha | \hat{A} | \alpha \rangle] \\
\|\hat{q}\vec{v}_\perp\|^2 &\rightarrow \text{Var}_{\text{GGE}}[\langle \alpha | \hat{I} | \alpha \rangle].
\end{aligned}$$

3. Several additional integrals of motion and a single observable of interest.

One can further introduce another integral of motion, \hat{I}_2 , orthogonal to the first one: $(\langle \hat{I}_2 | \hat{I}_\perp \rangle) = 0$. Introducing a fictitious observable with matrix elements $\langle \alpha | \hat{A} | \alpha \rangle - \text{Mean}_{\text{GGE} | j(\alpha)}[A]$, the bound (12) can be generalized to

$$\begin{aligned}
\text{MSE}[\text{Prediction}[\text{Mean}_t[A]]] &\equiv \text{Var}_{\text{GGE}}[\langle \alpha | \hat{A} | \alpha \rangle] \lesssim \\
&\text{Var}_{\text{MC}}[\langle \alpha | \hat{A} | \alpha \rangle] \times \\
&\left(1 - \cos^2[\theta_{\hat{I}_\perp, \hat{P}_H \hat{A}_\perp}] - \cos^2[\theta_{(\hat{I}_2)_\perp, \hat{P}_H \hat{A}_\perp}]\right).
\end{aligned}$$

Furthermore, by induction, one can extend this bound to any number N_I of (mutually orthogonal) integrals of motion:

$$\begin{aligned}
\text{MSE}[\text{Prediction}[\text{Mean}_t[A]]] &\equiv \text{Var}_{\text{GGE}}[\langle \alpha | \hat{A} | \alpha \rangle] \lesssim \\
&\text{Var}_{\text{MC}}[\langle \alpha | \hat{A} | \alpha \rangle] \left(1 - \sum_{m=1}^{N_I} \cos^2[\theta_{(\hat{I}_m)_\perp, \hat{P}_H \hat{A}_\perp}]\right).
\end{aligned}$$

For future applications, we will quote two other expressions for this bound:

$$\begin{aligned}
\text{MSE}[\text{Prediction}[\text{Mean}_t[A]]] &\equiv \text{Var}_{\text{GGE}}[\langle \alpha | \hat{A} | \alpha \rangle] \lesssim \quad (13) \\
&\text{Var}_{\text{MC}}[\langle \alpha | \hat{A} | \alpha \rangle] - \text{Var}_{\text{MC}}[A] \sum_{m=1}^{N_I} \cos^2[\theta_{(\hat{I}_m)_\perp, \hat{A}_\perp}],
\end{aligned}$$

where $\text{Var}_{\text{MC}}[A] \equiv \text{Mean}_{\text{MC}}[A^2] - \text{Mean}_{\text{MC}}[A]^2$; and

$$\begin{aligned}
\text{MSE}[\text{Prediction}[\text{Mean}_t[A]]] &\equiv \text{Var}_{\text{GGE}}[\langle \alpha | \hat{A} | \alpha \rangle] \lesssim \quad (14) \\
&\text{Var}_{\text{MC}}[A] \cos^2[\theta_{\mathcal{L}_{\perp, d-\hat{H}} / \text{Span}\{(\hat{I}_m)_\perp \mid m=1, \dots, N_I\}, \hat{A}_\perp}],
\end{aligned}$$

where $\mathcal{L}/\mathcal{L}_{\text{sub}}$ is the orthogonal complement of a subspace \mathcal{L}_{sub} of a vector space \mathcal{L} with respect to an inner product $(A|B)$ (the Frobenius or Hilbert-Schmidt product $(\hat{A}|\hat{B})$ in our case).

4. Several additional integrals of motion and several observables of interest.

Now, assume that we have several observables of interest (spanning a linear space $\mathcal{L}_{o.i.}$) whose long-term behavior we

want to be able to predict. Assume further that we are given several integrals of motion (spanning a space $\mathcal{L}_{I,\perp}$) we are allowed to use as thermodynamical predictors. Next, we are going to form linear spaces $\mathcal{L}_{o.i.,\perp}$ and $\mathcal{L}_{I,\perp}$ spanned by the traceless versions of the same observables. Now, let us introduce orthonormal bases for both spaces:

$$\begin{aligned}
&(\hat{A}_q)_\perp \quad \text{with } q = 1, 2, \dots, N_{o.i.} \\
&((\hat{A}_q)_\perp | (\hat{A}_{q'})_\perp) = \delta_{q,q'} \\
&(\hat{I}_m)_\perp \quad \text{with } m = 1, 2, \dots, N_I \\
&((\hat{I}_m)_\perp | (\hat{I}_{m'})_\perp) = \delta_{m,m'}.
\end{aligned}$$

In particular, this implies that $\text{Var}_{\text{MC}}[A_q] = \text{Var}_{\text{MC}}[I_m] = 1$ for all q and m . Let us now form the following matrix:

$$\begin{aligned}
R_{m,m'} &= \sum_{q=1}^{N_{o.i.}} \cos[\theta_{(\hat{I}_m)_\perp, (\hat{A}_q)_\perp}] \cos[\theta_{(\hat{A}_q)_\perp, (\hat{I}_{m'})_\perp}] \\
m, m' &= 1, 2, \dots, N_I,
\end{aligned}$$

cf. Eqn. 13.

It can be shown that the eigenvectors of $R_{m,m'}$, $\hat{I}_{\tilde{m}}$, when ordered in the descending order of their eigenvalues $r_{\tilde{m}}$ form a sequence such that the first $N_{\text{opt.}}$ members constitute the most optimal Generalized Gibbs Ensemble involving $N_{\text{opt.}}$ integrals, in the sense that it minimizes, on average, the error in the prediction of the ensemble. The requests for linear combinations of the observables of interest are supposed to be distributed according to a spherically symmetric probability distribution, with respect to the Hilbert-Schmidt measure.

We show examples of a relevance sequence in Figs. 3a and b. In the examples considered in Fig. 3, the space $\mathcal{L}_{I,\perp}$ was represented by the whole space of traceless integrals of motion $\mathcal{L}_{\perp, d-\hat{H}}$. The number of the most optimal (relevant) integrals of motion was 16 for both Fig. 3c and Fig. 3d.

5. The classical billiard with a soft-core scatterer.

The classical mechanics example considered in the letter consists of a two-dimensional particle of mass m , moving in a rectangular billiard with periodic boundary conditions (thus topologically equivalent to a torus). As an integrability-breaking perturbation, we use a ‘‘truncated’’ δ -function: a potential that consists of the first M (including the zeroth one) spatial harmonics of a δ -function (see Fig. 5). The resulting hamiltonian is

$$\begin{aligned}
H(x, y, p_x, p_y) &= \frac{p_x^2}{2m} + \frac{p_y^2}{2m} \\
&+ V \frac{\sin[2\pi(M+1/2)x/L] \sin[2\pi(M+1/2)y/L]}{(2M+1) \sin[\pi x/L] (2M+1) \sin[\pi y/L]},
\end{aligned}$$

where

$$\begin{aligned}
0 \leq x < L; \quad (x=L) &\equiv (x=0) \\
0 \leq y < L; \quad (y=L) &\equiv (y=0).
\end{aligned}$$

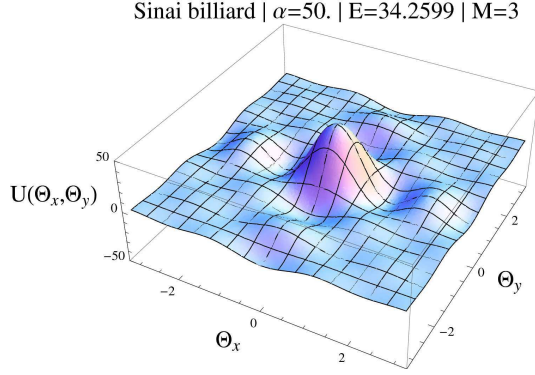


FIG. 5: **The integrability-breaking barrier for the classical system considered.** The plot shows the “truncated” δ -function potential used as an integrability-breaking perturbation acting on a particle in a two-dimensional square billiard.

In what follows, we will be using a system of units where $m = \frac{L}{2\pi} = 1$. The hamiltonian then becomes

$$H(\theta_x, \theta_y, I_x, I_y) = \frac{I_x^2}{2} + \frac{I_y^2}{2} + V \frac{\sin[(M + 1/2)\theta_x]}{(2M + 1) \sin[\theta_x/2]} \frac{\sin[(M + 1/2)\theta_y]}{(2M + 1) \sin[\theta_y/2]},$$

where, in this system of units, we have $I_\alpha = p_\alpha$ and $\theta_\alpha = r_\alpha$ ($\alpha = x, y$); also, $r_x \equiv x$; $r_y \equiv y$. We used $M = 3$ for all data points.

For any strength of the perturbation V , the initial conditions were drawn from a microcanonical ensemble bounded by the equi-energy surfaces (specific for a given V) in such a way that the phase-space volume below the lower surface was $W_b = 7895.7$, and in between the lower and the upper was $W = 1184.3$, regardless of the perturbation strength. A quantum-mechanical analogue of such an ensemble would have the same lower and upper quantum indices of the microcanonical window for all realizations. To give the reader an idea of the energy scale involved, we will note that for a zero barrier height, the mean energy in the ensemble is $E_0 = 33.7$.

For the test observable A , we used the difference between the kinetic energies in the x - and y -directions: $A = \Delta E_{\text{kin.}} \equiv \frac{p_x^2}{2m} - \frac{p_y^2}{2m}$ (which is $\frac{I_x^2}{2} - \frac{I_y^2}{2}$ in our system of units). We studied both the ensemble variance of the temporal mean,

$$\text{Var}_{\text{MC}}[\text{Mean}_t[A]] \equiv \frac{\int_{\text{MC}} d\theta_x^{t=0} d\theta_y^{t=0} dI_x^{t=0} dI_y^{t=0} \left\{ \left(\lim_{t_{\text{max}} \rightarrow \infty} \frac{1}{t_{\text{max}}} \int_{t=0}^{t_{\text{max}}} dt A(t) \right) - \text{Mean}_{\text{MC}}[A] \right\}^2}{\int_{\text{MC}} d\theta_x d\theta_y dI_x dI_y 1}, \quad (15)$$

and the ensemble mean of the temporal variance,

$$\text{Mean}_{\text{MC}}[\text{Var}_t[A]] \equiv \frac{\int_{\text{MC}} d\theta_x^{t=0} d\theta_y^{t=0} dI_x^{t=0} dI_y^{t=0} \lim_{t_{\text{max}} \rightarrow \infty} \frac{1}{t_{\text{max}}} \int_{t=0}^{t_{\text{max}}} dt \left\{ A(t) - \left(\lim_{t_{\text{max}} \rightarrow \infty} \frac{1}{t_{\text{max}}} \int_{t'=0}^{t_{\text{max}}} dt' A(t') \right) \right\}^2}{\int_{\text{MC}} d\theta_x d\theta_y dI_x dI_y 1},$$

where the ensemble average is

$$\text{Mean}_{\text{MC}}[A] \equiv \frac{\int_{\text{MC}} d\theta_x d\theta_y dI_x dI_y A}{\int_{\text{MC}} d\theta_x d\theta_y dI_x dI_y 1},$$

$\int_{\text{MC}} d\theta_x d\theta_y dI_x dI_y \dots$ is an integral over the microcanonical volume describe above, and $A(t)$ the time dependence for the observable A along a trajectory that starts at $(\theta_x^{t=0}, \theta_y^{t=0}, I_x^{t=0}, I_y^{t=0})$.

6. The hamiltonian for one-dimensional hard-core bosons perturbed by soft-core interactions.

The quantum hamiltonian used in this Letter reads

$$\hat{H} = -J \sum_j (\hat{b}_j^\dagger \hat{b}_{j+1} + \text{h.c.}) + \frac{1}{2} \sum_{j_1} \sum_{j_2} V(j_1, j_2) \hat{b}_{j_1}^\dagger \hat{b}_{j_2}^\dagger \hat{b}_1 \hat{b}_2, \quad (16)$$

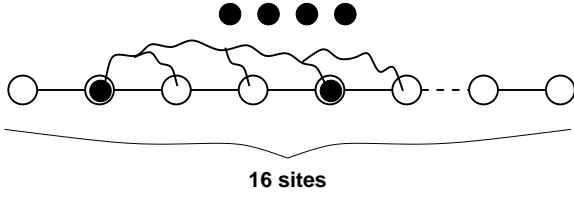


FIG. 6: **The lattice configuration for the quantum system considered.** One-dimensional hard-core bosons on a lattice with $L = 16$ sites. The number of atoms was 4 for the system of Fig. 1b and 3 for the system of Fig. 3. Open boundary conditions were imposed on the former system and periodic ones on the latter. The integrability-breaking perturbation was an added two-body interaction: a constant potential energy U for any two atoms separated by four sites or less.

where the commutation relations for the hard-core boson creation and annihilation operators obey

$$[b_j, b_{j'}^\dagger] = [b_j, b_{j'}] = [b_j^\dagger, b_{j'}^\dagger] = 0, \quad \text{for } j' \neq j$$

$$[b_j, b_j^\dagger] = 1, \quad (b_j^\dagger)^2 = (b_j)^2 = 0.$$

The soft-core interaction potential we used was a rectangular potential of a four-site range:

$$V(j_1, j_2) = U \begin{cases} 1 & \text{for } |j_2 - j_1| \leq \Delta j_{\text{range}} \\ 0 & \text{otherwise} \end{cases},$$

with $\Delta j_{\text{range}} = 4$ (see Fig. 6).

For the calculations resulting in Fig. 1b, the open boundary conditions were used: the first sum in Eq. (16) was extended to a range between $j = 1$ and $j = L - 1$, where $L = 16$ was the length of the lattice. Both sums in the second double sum were fixed between $j_{1,2} = 1$ and $j_{1,2} = L$.

The calculations that led to Fig. 3 were performed using periodic boundary conditions. There, the first sum involved in Eq. (16) covers all sites, from $j = 1$ to $j = L$. In the second sum, the index j_1 covers the same range, from $j_1 = 1$ to $j_1 = L$; the second index, j_2 , ranges from $j_2 = 1 - \Delta j_{\text{range}}$ to $j_2 = L + \Delta j_{\text{range}}$, so that the soft-core potential respects the periodic boundary conditions.

Also, in both cases, a weak random on-site perturbation was used,

$$W \sum_j \xi_j (\hat{b}_j^\dagger \hat{b}_j),$$

where $\{\xi_j\}$ is a set of independent random variables uniformly distributed between -1 and $+1$, and the strength of the potential was fixed to $W = 10^{-4}$. The strength W has been chosen in such a way that it remains weak enough not to alter any of the macroscopic properties, but strong enough to lift all possible degeneracies and, in the periodic case, to relax the selection rules associated with the translational invariance.

7. Quantum observables presented in Fig. 1b.

In Fig. 1b we analyze the properties of two integrals of motion, which are, in the case of a lattice with open

boundary conditions, related to the counterparts of the fourth and sixth moments of the momentum distribution of the underlying free fermions. When expressed through the bosonic creation and annihilation operators, the functionals of the fermionic momentum distribution—quadratic in the fermionic representation—become complicated many-body observables, such as

$$\hat{I}_4 = (1/2L) \sum_{j=1}^{L-2} ((\hat{b}_j^\dagger \hat{b}_{j+2} + \text{h.c.})$$

$$- 2(\hat{b}_j^\dagger \hat{b}_{j+1} \hat{b}_{j+1}^\dagger \hat{b}_{j+2} + \hat{b}_{j+2}^\dagger \hat{b}_{j+1} \hat{b}_{j+1}^\dagger \hat{b}_j)$$

$$- (\hat{b}_1^\dagger \hat{b}_1 + \hat{b}_L^\dagger \hat{b}_L)).$$

The second term inside the sum (the four-body one) is absent in the fermionic representation. The last term, present in both representations, is responsible for the finite size effects originating, in turn, from the open boundary conditions.

We also studied a “generic” integral of motion: $\hat{I}_{\text{random}} = \sum_{\alpha_0} \xi_{\alpha_0} |\alpha_0\rangle \langle \alpha_0|$, where the states $|\alpha_0\rangle$ are the eigenstates of the hamiltonian in Eq. (16) in the absence of the integrability-breaking perturbation, and the independent random coefficients ξ_{α_0} were uniformly distributed between -1 and $+1$.

8. Quantum observables presented in Fig. 3.

In Fig. 3, we are comparing three thermodynamic ensembles: the microcanonical ensemble (which is based on the energy alone),

$$\mathcal{L}_{\text{o.i.}} = \text{Span}\{\{\hat{H}\}\},$$

the conventional generalized Gibbs ensemble [5] (which is based on the occupation numbers of all free-fermionic one-body orbitals, or, in the case of periodic boundary conditions, all moments of the fermionic momentum distribution),

$$\mathcal{L}_{\text{o.i.}} = \text{Span} \left[\left\{ \frac{1}{2L} \sum_{j=1}^L ((\hat{a}_j^\dagger \hat{a}_{j+m} + \text{h.c.})), \right. \right.$$

$$\left. \left. \frac{-i}{2L} \sum_{j=1}^L ((\hat{a}_j^\dagger \hat{a}_{j+m} - \text{h.c.})) \mid m = 1, \dots, L/2 \right\} \right],$$

and the optimized generalized Gibbs ensemble (which is designed to maximize the quality of prediction for one-body observables),

$$\mathcal{L}_{\text{o.i.}} = \text{Span} \left[\left\{ \frac{1}{2} (\hat{b}_{j'}^\dagger \hat{b}_j + \text{h.c.}), \right. \right.$$

$$\left. \left. \frac{-i}{2} (\hat{b}_{j'}^\dagger \hat{b}_j - \text{h.c.}) \mid j = 1, \dots, L; j' = j, \dots, L \right\} \right].$$

Only the first few most optimal integrals of motion generated by the latter space were used. Here \hat{a}_j are the free-fermionic

annihilation operators, related to their bosonic counterparts via a Jordan-Wigner map, $\hat{a}_j = \left(\prod_{j'=1}^{j-1} e^{i\pi \hat{b}_{j'}^\dagger \hat{b}_{j'}} \right) \hat{b}_j$. Here and below, we are assuming that the number of sites L is even.

To compare the predictive powers of these ensembles, we compute their predictions for the momentum distribution of the bosons,

$$\hat{A}_m = \frac{1}{2L} \sum_{j=1}^L (\hat{b}_j^\dagger \hat{b}_{j+m} + \text{h.c.})$$

$$m = 1, \dots, L/2.$$

-
- [1] Deutsch, J. M. Quantum statistical mechanics in a closed system. *Phys. Rev. A* **43**, 2046–2049 (1991).
- [2] Srednicki, M. Chaos and quantum thermalization. *Phys. Rev. E* **50**, 888–901 (1994).
- [3] Rigol, M., Dunjko, V. & Olshanii, M. Thermalization and its mechanism for generic isolated quantum systems. *Nature* **452**, 854–858 (2008).
- [4] Santos, L. F. & Rigol, M. Onset of quantum chaos in one-dimensional bosonic and fermionic systems and its relation to thermalization. *Phys. Rev. E* **81**, 036206 (2009).
- [5] Rigol, M., Dunjko, V., Yurovsky, V. & Olshanii, M. Relaxation in a completely integrable many-body quantum system: An ab initio study of the dynamics of the highly excited states of 1D lattice hard-core bosons. *Phys. Rev. Lett.* **98**, 050405 (2007).
- [6] Amy C. Cassidy, M. R., Charles W. Clark. Generalized thermalization in an integrable lattice system. *Phys. Rev. Lett.* **106**, 140405 (2011).
- [7] Marcus Kollar, M. E., F. Alexander Wolf. Generalized Gibbs ensemble prediction of prethermalization plateaus and their relation to nonthermal steady states in integrable systems. *Phys. Rev. B* **84**, 054304 (2011).
- [8] Gring, M. *et al.* Relaxation and prethermalization in an isolated quantum system. *Science* **337**, 1318–1322 (2012).
- [9] Gramsch, C. & Rigol, M. Quenches in a quasidisordered integrable lattice system: Dynamics and statistical description of observables after relaxation. *Phys. Rev. A* **86**, 053615 (2012).
- [10] See the Methods section.
- [11] Srednicki, M. Thermal fluctuations in quantized chaotic systems. *J. Phys. A* **29**, L75 (1996).
- [12] Girardeau, M. Relationship between systems of impenetrable bosons and fermions in one dimension. *J. Math. Phys.* **1**, 516–523 (1960).
- [13] Georgeot, B. & Shepelyansky, D. L. Breit-Wigner width and inverse participation ratio in finite interacting Fermi systems. *Phys. Rev. Lett.* **79**, 4365–4368 (1997).
- [14] Olshanii, M. *et al.* An exactly solvable model for the integrability chaos transition in rough quantum billiards. *Nat. Commun.* **3**, 641 (2012).
- [15] Cazalilla, M. A. Effect of suddenly turning on interactions in the Luttinger model. *Phys. Rev. Lett.* **97**, 156403 (2006).
- [16] Gaudin, M. *La fonction d'onde de Bethe* (Masson, Paris; New York, 1983).
- [17] Sutherland, B. *Beautiful Models: 70 Years of Exactly Solved Quantum Many-Body Problems* (World Scientific, Singapore, 2004).
- [18] Teufel, J. D. *et al.* Sideband cooling of micromechanical motion to the quantum ground state. *Nature* **475**, 359 (2011).
- [19] Chan, J. *et al.* Laser cooling of a nanomechanical oscillator into its quantum ground state. *Nature* **478**, 89 (2011).
- [20] Verhagen, E. *et al.* Quantum-coherent coupling of a mechanical oscillator to an optical cavity mode. *Nature* **482**, 63 (2012).
- [21] O’Connell, A. D. *et al.* Quantum ground state and single-phonon control of a mechanical resonator. *Nature* **464**, 697 (2010).
- [22] Groblacher, S., Hammerer, K., Vanner, M. R. & Aspelmeyer, M. Observation of strong coupling between a micromechanical resonator and an optical cavity field. *Nature* **460**, 724 (2009).
- [23] Teufel, J. D. *et al.* Circuit cavity electromechanics in the strong-coupling regime. *Nature* **471**, 204 (2011).
- [24] Aspelmeyer, M., Meystre, P. & Schwab, K. Quantum optomechanics. *Physics Today* **65**, 29 (2012).

Acknowledgements The author thanks Marcos Rigol, David Weiss, Vanja Dunjko, Alessandro Silva, and Bala Sundaram for comments. This work was supported by the US National Science Foundation Grant No. PHY-1019197, the Office of Naval Research Grants No. N00014-09-1-0502 and N00014-12-1-0400, and a grant from the *Institut Francilien de Recherche sur les Atomes Froids* (IFRAF). Support from the *Laboratoire de Physique des Lasers* of Paris 13 University is also appreciated.

Author contributions All work was done by M.O.

Additional information Supplementary information is available in the online version of the paper. Reprints and permissions information is available online at www.nature.com/reprints. Correspondence and requests for materials should be addressed to M.O.

Competing financial interests The author declares no competing financial interests.